PERIODICA POLYTECHNICA SER. EL. ENG. VOL. 34, NO. 1, PP. 55-71 (1990)

THE HIGH ELECTRON MOBILITY TRANSISTOR (HEMT) — PHYSICAL FUNDAMENTALS AND QUASI TWO-DIMENSIONAL (Q2D) SIMULATION

CH. SCHNITTLER, G. HOLZ

Sektion Physik und Technik Elektronischer Bauelemente,
Wissenschaftsbereich Physik
Technische Hochschule
Ilmenau, DDR

Received Febr. 5, 1989.

Abstract

Construction, function, and physical fundamentals of the high electron mobility transistor (HEMT) are shortly reviewed. It is the main feature of a semiconductor heterostructure of this type that a 2D electron gas occurs which demands a careful consideration of quantum size effects. For doing this with a moderate numerical expense, a very convenient method is proposed which is basically a modification of the well-known Thomas–Fermi approximation for potentials with steps. By means of this method a quasi-2D simulation of the standard HEMT is carried out. First the electronic properties of the HEMT without a source-drain voltage are determined. Assuming a suitable semi-empirical mobility model, the current–voltage characteristics are calculated, too, without using any fitting parameters. The influence of geometrical and material parameters as well as of the temperature and doping on the electronic properties of the HEMT is discussed.

Keywords: III-V semiconductors, HEMT

Introduction: Heterostructures and new device concepts

In the recent years a new class of microelectronic devices, based on semiconductor heterostructures, has been developed for special applications. For manufacturing such devices usually compound semiconductors of the III/IV-type are used: binary (GaAs, GaSb, InSb, InP), ternary (AlGaAs, CdHgSe) and even quaternary semiconductors (InGaAsP). The advantage of such materials is the high electron mobility and the possibility to modify the band gap and/or the lattice constant by changing the chemical composition.

The most characteristic common property of such devices is the significance of the heterointerface which can be prepared nearly atomically abrupt by modern techniques as molecular beam epitaxy (MBE) and metal organic chemical vapour deposition (MOCVD). So Kroemer (KROEMER, 1983) made the striking statement that preparation of high performance semiconductor devices means minimizing the non-active part of the device volume 'to the point that the device turns from a collection of semicon-

ductor regions separated by interfaces to a collection of interfaces with a minimum of semiconductor between them'.

Because of the different band gaps of two materials, discontinuities ('band offsets') occur in both the conduction and valence bands at the heterointerface. They influence the electronic structure of such heterosystems drastically and give possibility to use quite new effects and principles for device operation. The most interesting of this type are the compositional superlattices. Here we deal with a more easy example which is on the market and technically used for realizing very short delay times down to some ps: the *h*igh *e*lectron *m*obility *t*ransistor (HEMT), sometimes also called MODFET, TEGFET, or SDHT (MIMURA ET AL., 1980; MORKOC and SOLOMON, 1984.)

Construction and function of the standard HEMT

In *Fig. 1.* a cross-sectional view of the standard HEMT is shown.

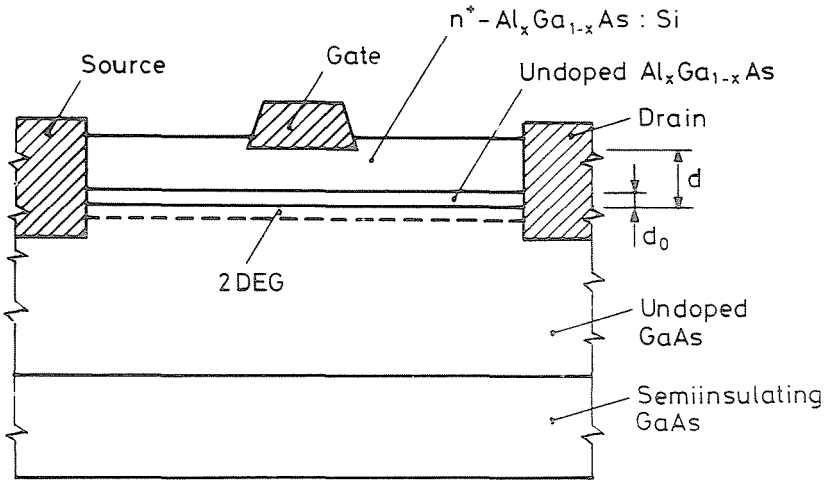

Fig. 1. Structure of the standard HEMT (cross-section, schematically).

On a semi-insulating chromium-compensated GaAs substrate an undoped highly pure GaAs layer is grown (thickness is about 1 μm) in the upper part of which (the 'channel') the electron transport between source and drain occurs. Then a very thin intrinsic $Al_xGa_{1-x}As$ layer, the spacer (thickness $d_0 = 2...20$ nm), and thicker highly Si–doped n^+-$Al_xGa_{1-x}As$ layer (thickness $d - d_0 = 20...60$ nm) with an Al content of about 0.3 follow. On the

top of the structure is the gate contact consisting of a layer sequence titanium/platinum/gold where the closing gold layer determines the Schottky barrier height ΔE_B. The ohmic source and drain contacts are realized by a gold/germanium/nickel alloy giving a very good ohmic contact to the channel because of the deep diffusion of the Ge atoms.

The heterointerface $Al_xGa_{1-x}As/GaAs$ is fundamental for the function of the HEMT. Because of the larger band gap of $Al_xGa_{1-x}As$ (depending on x), a band offset ΔE_C of about 225 meV (for $x = 0.3$) occurs. Due to the difference of the work functions electrons are transferred from n^+-$Al_xGa_{1-x}As$ to GaAs causing a typical band bending. The conduction band edge $E_C(z)$ versus distance z from the heterointerface is given in *Fig. 2.* The spacer serves only for a better separation of the ionized donors, remaining in the $Al_xGa_{1-x}As$, from the electrons collected in the channel where $E_C(z)$ decrease below the Fermi level E_F.

From *Fig. 2.* it is easy to recognize to main advantages of the HEMT: (i) The electron transport occurs in the GaAs using the large electron mobility of about 8500 cm^2/Vs already at room temperature.

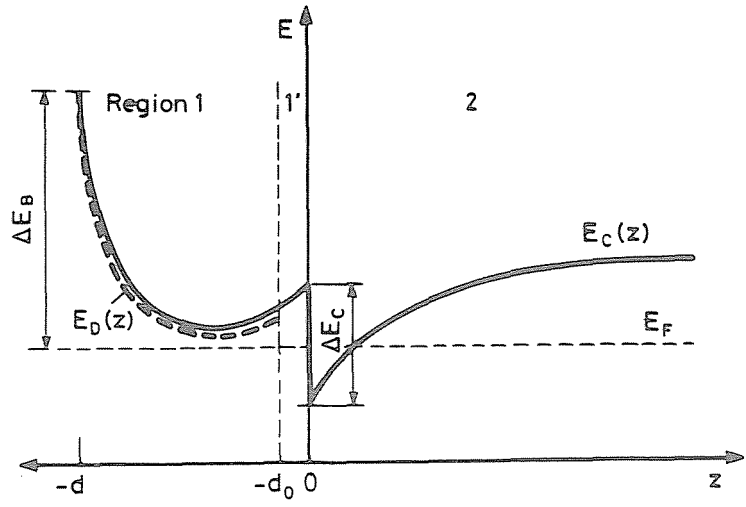

Fig. 2. Typical conduction band diagram of the standard HEMT (1: n-doped $Al_xGa_{1-x}As$; 1': undoped $Al_xGa_{1-x}As$; 2: undoped GaAs)

(ii) Due to the geometry the channel electrons are separated from the ionized donors acting as scattering centres. This spatial separation can be improved by introducing a spacer which is, however, not essential for device operation. (iii) By additional cooling down to the temperature of liquid nitrogen, the electron mobility in the channel can be increased

up to 10^5 cm^2/Vs. This is possible due to the strongly reduced phonon scattering.

Like in normal MIS transistor the charge in the channel is controlled by the gate voltage. In the case of *Fig. 2.* channel occurs already in the unbiassed transistor; so we have a normally-on HEMT which can be switched off by a negative gate voltage. The condition for such a behaviour is a sufficient amount of donors, which means, first of all, a sufficient thickness of the n^+-$Al_xGa_{1-x}As$ layer. From this a further important advantage of the HEMT becomes obvious: by decreasing the value of $d - d_0$ a second type of transistor can be produced by the same technology, which does not have a conducting channel in the unbiassed state. This so-called normally-off HEMT can be switched on by a positive gate voltage.

We want to note that the standard HEMT has deficiencies, too, which can be avoided, to a great extent, by other HEMT modifications. One of the most favourable modifications is the insulated-gate inverted-structure or I^2-HEMT (KINOSHITA et al., 1986.) with a layer sequence i-$Al_xGa_{1-x}As$ /i-GaAs/n^+-$Al_xGa_{1-x}As$.

The new physical situation: occurrence of a two-dimensional (2D) electron gas

Due to the nearly triangular potential well in the GaAs layer near to the heterojunction, the electron motion, being free in a plane parallel to the interface, is strongly restricted in the z-direction. So in semiconductor heterostructures like the HEMT a new physical situation arises: the electrons in the channel form a 2D electron gas. As a consequence, a new type of band structure occurs: the so-called 2D subband structure, shown schematically in *Fig. 3.*

By separating the Schrödinger equation, the wave functions can be written in the form

$$\Psi(x, y, z) = (L_x L_y)^{-1/2} \exp[i(k_x x + k_y y)] \chi_n(z) \tag{1}$$

with a normalization area $L_x L_y$ in the (x, y)-plane. From this an energy spectrum

$$E_n(k_x, k_y) = \frac{\hbar^2 (k_x^2 + k_y^2)}{2m^*} + \epsilon_n = \frac{\hbar^2 k_\rho^2}{2m^*} + \epsilon_n \tag{2}$$

is derived consisting of parabolic subbands E_n with discrete subband levels, and ϵ_n is the 'bottom' of these bands. The corresponding local density of

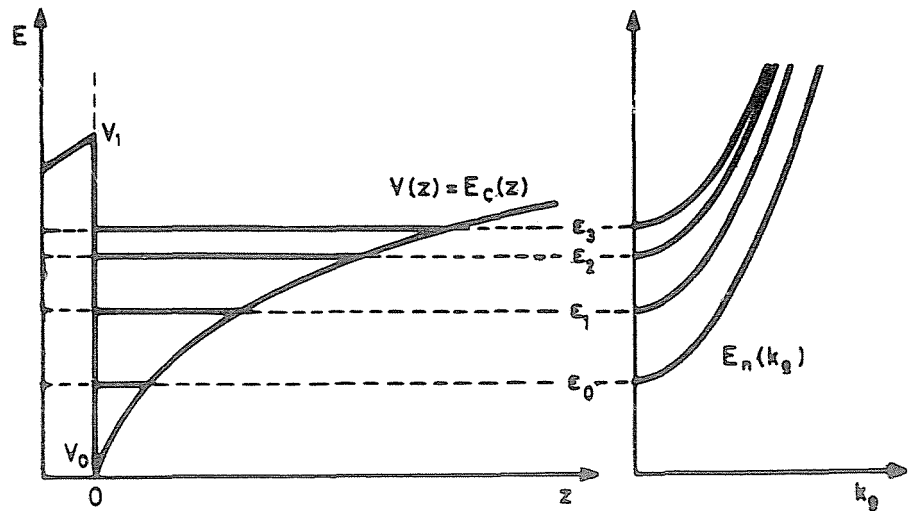

Fig. 3. Typical subband levels and corresponding energy spectrum for electrons near a heterointerface at $z = 0$

states $D(z, E)$ is a stepped function with respect to the energy E:

$$D(z, E) = \frac{m^*}{\pi n^2} \sum_n |\chi_n(z)|^2 H(E - \epsilon_n) \tag{3}$$

(H: Heaviside function).

Such kind of quantum size effects are essential for the electronic properties of the HEMT and are much more important than for traditional MIS transistors based on silicon. The reason for this is the small effective mass

$$m^* = 0.068 \cdot m_0 \tag{4}$$

(m_0: free electron mass) of GaAs producing a large spacing of the subband levels and so very distinct effects of the subband structure. As a consequence, in GaAs the channel electrons are concentrated in the two lowest subbands only, even at room temperature.

So the problem arises how to simulate the HEMT or a similar heterostructure considering the properties of the 2D electron gas. For this simultaneous and self-consistent solution of the Schrödinger and the Poisson equations is necessary (HOLZ, 1988). Though this is not a problem today, a large expense of computing time is necessary, and such a complicated procedure is very inappropriate for device simulation. Therefore we propose a suitable approximation method which works very exactly and allows a simulation nearly as easy as that without considering quantum size effects.

The modified Thomas–Fermi approximation

For the electron density n in a semiconductor with the Fermi level E_F, temperature T, and effective density of states N_C in the conduction band the well-known formula

$$n = \frac{2N_C}{\sqrt{\pi}} F_{1/2}\left(\frac{E_F - E_C}{k_B T}\right) \tag{5}$$

holds ($F_{1/2}$: Fermi integral of the order 1/2). Originally (5) was derived for a homogeneous semiconductor with a space independent value of E_C.

In the case of an inhomogeneous semiconductor with a macroscopic electric potential $\varphi(z)$ the model of bent bands with

$$E_C(z) = E_C^0 - e\varphi(z) = V(z) \tag{6}$$

($e > 0$: elementary charge) is used. The common Thomas–Fermi approximation says that for relatively smooth potentials $\varphi(z)$ a local electron density $n(z)$ can be calculated by inserting (6) into (5).

For a heterostructure the condition of a smooth potential is extremely violated at the interface. Our basic idea is to extend the Thomas–Fermi approximation to potentials with steps due to band offsets. First of all this has been done for an infinite potential step by means of an appropriate modification of the completeness relation according to the right-side boundary conditions (PAASCH, 1981; PAASCH and ÜBENSEE, 1982). Recently a more general method has been developed (TROTT and SCHNITTLER, 1989) including, in a systematic manner, also finite steps.

The result of such a modified Thomas–Fermi approximation is a modified local density of states containing the effects of the 2D electron gas. As an example, in the most easy case of an infinite potential step at $z = 0$, the density of states is

$$D(z, E) = D_b(z, E)\left\{1 - \frac{\sin[2zk(z)]}{2zk(z)}\right\} \tag{7}$$

with the bulk value

$$D_b(z, E) = \frac{m^* k(z)}{\pi^2 \hbar^2} = \frac{m^* \sqrt{2m^*(E - V(z))}}{\pi^2 \hbar^3} \tag{8}$$

The correction factor in the braces in (7) becomes zero for $z = 0$ and tends to 1 in the bulk describing the attenuation of the wave functions towards the heterointerface.

Now, with an expression of the type (7), it is sufficient to solve the Poisson equation one time only. Then from $V(z)$, the electron density $n(z)$ can be calculated as

$$n(z) = \int_{V(z)}^{\infty} dE \quad D(z,E) \cdot f(E - E_F) \tag{9}$$

(f: Fermi–Dirac distribution) without solving the Schrödinger equation. This procedure is very easy, it is of high accuracy, and therefore very convenient for device simulation.

Thomas–Fermi approximation and parameters for the standard HEMT

Simulating the standard HEMT in this way, the Poisson equation with consideration of (6)

$$\frac{d^2V(z)}{dz^2} = \frac{e^2}{\varepsilon_0 \varepsilon_r}\left[N_D^+(z) - n(z)\right] \tag{10}$$

has to be solved throughout the whole structure. In region 2 of *Fig. 2.* ($z > 0$, GaAs) the Thomas–Fermi expression for the electron density is

$$n_2(z) = \frac{2N_{C2}}{\sqrt{\pi}} \int_0^{\infty} \frac{dE\sqrt{E}\left\{1 - \dfrac{\sin[2(z+z_0)\sqrt{E}/L]}{2(z+z_0)\sqrt{E}/L}\right\}}{1 + \exp\left\{\dfrac{E - [E_F - V(z)]}{k_B T}\right\}} \tag{11}$$

The characteristic length

$$L = \hbar/\sqrt{2m_2^* k_B T} = (4N_{C2})^{-1/3} \cdot \pi^{-1/2} \tag{12}$$

is essentially the de Broglie wave length of the electrons in GaAs. A further characteristic length

$$z_0 = \hbar/\sqrt{2m_2^* t_m \cdot \Delta E_C} \tag{13}$$

is introduced for considering the finite height ΔE_C of the potential step, and the parameter

$$t_m = m_2^*/m_1^* \tag{14}$$

is due to the different effective masses in GaAs and in $Al_xGa_{1-x}As$.

In region 1 of *Fig. 2.* ($z < 0$, $Al_xGa_{1-x}As$) the electron density is approximately

$$n_{1(z)} = \frac{2N_{C1}}{\sqrt{\pi}} F_{1/2}\left(\frac{E_F - V(z)}{k_B T}\right) + \frac{4N_{C2} k_B T}{3\sqrt{\pi} t_m \cdot \Delta E_C} F_{3/2}\left(\frac{E_F - V_0}{k_B T}\right) \exp\left[\frac{2z}{\hbar}\sqrt{2m_1^* \cdot (V(z) - V_0)}\right] \tag{15}$$

with $V_0 = V(+0)$ as the 'bottom' of the triangular potential well. The first part of (15) is the usual bulk electron density in $Al_xGa_{1-x}As$; the second term is due to the tunnelling of electrons from the GaAs into the barrier. $F_{3/2}$ is the Fermi integral of the order 3/2. Additionally, the correct Fermi–Dirac expression for the density of ionized donors

$$N_D^+(z) = \frac{N_D}{1 + 2 \cdot exp\left\{\left[E_F - E_D - V(z))\right]/k_B T\right\}} \tag{16}$$

is to be used.

Solving the Poisson equation (10) with (11)-(16), a considerable number of parameters have to be specified. These are first the geometrical parameters d and d_0. As energy parameters, the Fermi level E_F (relative to E_C in the bulk), the donor level E_D (relative to E_C), the band offset ΔE_C, and the Schottky barrier height ΔE_B are relevant. An exact determination of these quantities is not quite easy. The real value of ΔE_C, for instance, has been in discussion for a long time (SCHNITTLER, 1988). ΔE_C as well as ΔE_B are also dependent on technological conditions. A further important parameter is the donor concentration N_D, whereas the temperature T is of minor influence on the equilibrium properties of the HEMT. The dielectric constants ε_r of the materials are well known.

Electronic properties of the unbiassed HEMT

Under equilibrium conditions, the electron sheet concentration

$$n_S = \int_0^\infty \left[n(z) - n_{FB}(z)\right] dz \tag{17}$$

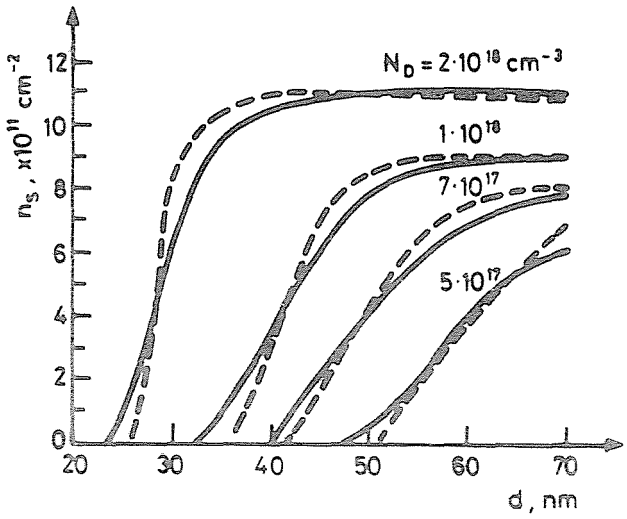

Fig. 4. Sheet concentration n_S versus thickness d of the $Al_xGa_{1-x}As$ layer for $d_{0=0}$ and different values of the donor concentration N_D; T: 300 K (—) and 77 K (- - -)

is the most interesting quantity. $n_{FB}(z)$ is the electron concentration which occurs in the GaAs layer in the case of flat bands; in the channel is always $n_{FB} \ll n$.

In *Fig. 4.*, n_S is given as a function of the total thickness d of the $Al_xGa_{1-x}As$ layer for different values of the donor concentration N_D.

In a relatively small range, n_S is strongly increasing with d; there the electronic properties of the HEMT are essentially determined by the precision of device manufacturing. Above a certain value of d, the influence of the Schottky barrier vanishes and n_S reaches a saturation value determined by the heterointerface itself without a neighbouring Schottky gate.

The donor concentration N_D is of great influence on n_S. With increasing N_D the saturation begins at a lower value of d and the saturation value of n_S becomes higher. The influence of the temperature T, on the other hand, is relatively small. Only the saturation behaviour becomes more distinct if T decreases considerably below room temperature.

The influence of spacer thickness d_0 on n_S is shown in *Fig. 5.* for a fixed value of d and different values of N_D, again. With increasing d_0 the sheet concentration, of course, decreases monotonously; so the advantage of the lowered Coulomb scattering of the channel electrons is compensated more and more. Actually, the influence of the spacer is more involved because of the complicated scattering behaviour. Therefore, to choose a proper spacer thickness is a difficult optimization problem.

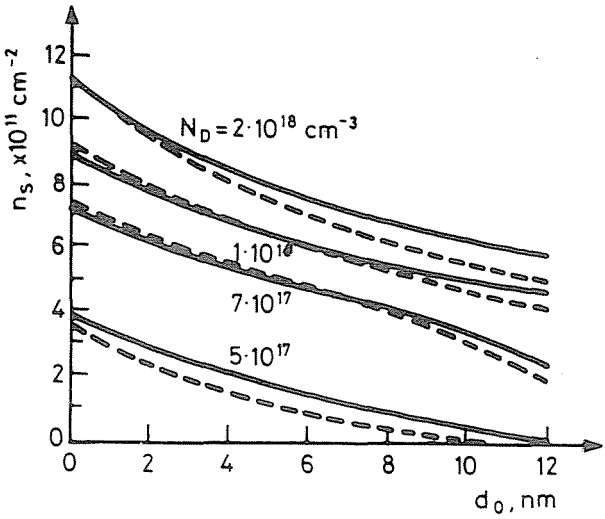

Fig. 5. Sheet concentration n_S versus thickness d_0 of the spacer for d=60 nm and different values of the donor concentration N_D; T: 300 K(—) and 77K (- - -)

Moreover, the function $n_S(d_0)$ strongly depends on d, too (HOLZ, 1988). The temperature, again, has relatively small influence down to the liquid nitrogen temperature.

For the dependence of n_S on d the real value of ΔE_C is essential. This is shown in *Fig. 6.* for two limiting cases described in the literature.For a given donor concentration, the upper curves are for $\Delta E_C = 0.85 \cdot \Delta E_G$ which has been accepted as Dingle's rule for nearly ten years (DINGLE et al., 1975). Today the lower value, $\Delta E_C \approx 0.6 \cdot \Delta E_G$, reported first by Miller from measurements on specially prepared superlattices (MILLER et al., 1984), is known to be more realistic. It results in considerably lower saturation values of n_S.

Charge control by the gate voltage

For all types of the HEMT channel charge is controlled by the gate–source voltage U_{GS}. In calculating the electronic properties for $U_{GS} = 0$ we have to consider the changed boundary condition at the Schottky contact only:

$$E_C(-d) = V(-d) = \Delta E_B - eU_{GS} \tag{18}$$

Here an additional difficulty arises: $Al_xGa_{1-x}As$ is not so well insulating as, e.g. SiO_2 in a common MIS transistor. Therefore a gate leakage current

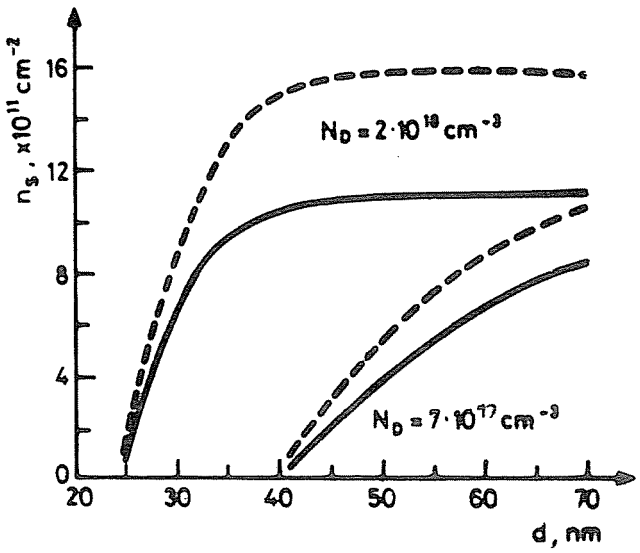

Fig. 6. Sheet concentration n_S versus thickness d of the $Al_xGa_{1-x}As$ layer for $\Delta E_C = 0.6 \cdot \Delta E_G$ (—) and $\Delta E_C = 0.85 \cdot \Delta E_G$ (- - -) and for two different values of the donor concentration N_D

may be possible, the value of which is spatially constant and is determined by the gradient of a quasi-Fermi level E_F^* as the 'driving force':

$$j_n = e \cdot \mu_n(z) \cdot n(z) \cdot dE_F^*/dz \tag{19}$$

where μ_n is the electron mobility in $Al_xGa_{1-x}As$.

The variation of the conducting band edge E_C and the quasi-Fermi level E_F^* with the distance z from the interface is given in *Fig. 7.*

For a negative gate-source voltage, no measurable leakage current can flow. E_F^* is practically constant through all semiconductor layers and rises to its value in the gate immediately in front of the metal-semiconductor interface. For positive values of U_{GS}, however, the conduction band edge in $Al_xGA_{1-x}As$ is moved down. Then we may have a remarkable electron concentration and a strongly variable quasi-Fermi level in $Al_xGa_{1-x}As$. A more detailed analysis shows that a gate leakage current has to be considered if U_{GS} is near to about +1 V (HOLZ, 1988).

The sheet concentration versus U_{GS} function is shown in *Fig. 8.* for different values of d. For larger values of d a saturation behaviour is visible which is more distinct in the case of lower temperatures. Only in the region of the steep increase on n_S with U_{GS}, depending strongly on d, is an effective charge control possible. In this region the charge control is supported by

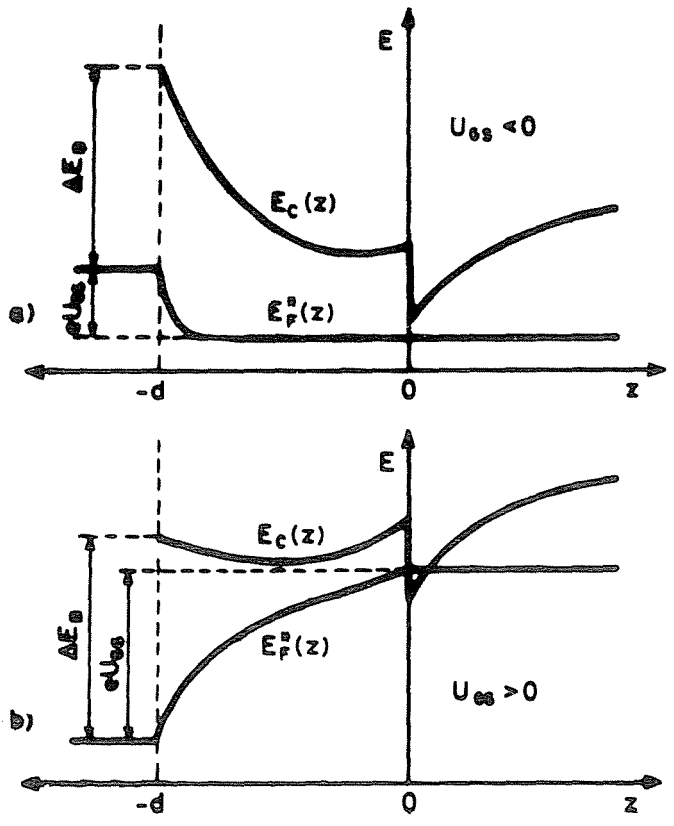

Fig. 7. Conduction band edge E_C and quasi-Fermi level E_F^* versus z for a negative (a) and a positive (b) gate-source voltage, U_{GS}

low temperatures. For a gate voltage $U_{GS} > 0.8$ V a variable quasi-Fermi level has to be considered giving practically a breakdown of the Schottky contact.

A semi-empirical model for the electron mobility in GaAs

For simulating the current-voltage characteristics of a HEMT, a model for the electron mobility in GaAs is necessary. This is a very complicated problem because of the considerable number of (at least 8) different scattering mechanisms, the involved nature of each single mechanism, and the existence of two 'ways' for scattering, intra- and intersubband scatterings (WALUKIEWICZ et al., 1984; STÖRMER, 1984). But for device simulation we need a mobility model of limited complexity. For this usually three

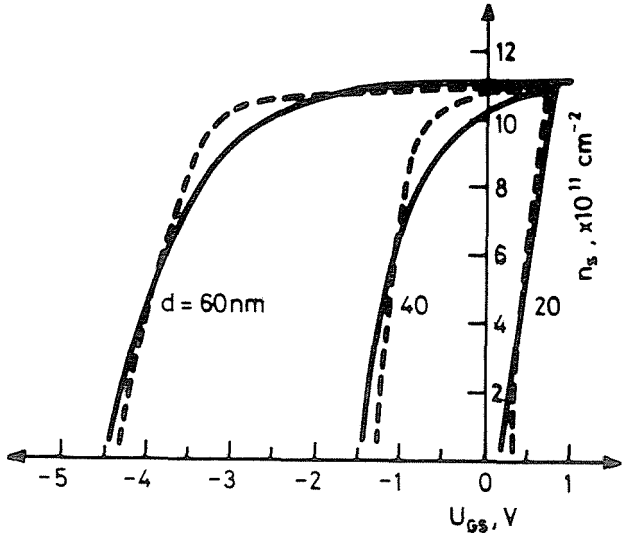

Fig. 8. Sheet concentration n_S versus gate-source voltage U_{GS} for $N_D = 2 \cdot 10^{18}$ cm^{-3} and different values of d; T: 300 K (—) and 77 K(- - -)

approximations are introduced:
(i) Only the most important scattering mechanisms are considered, that is, scattering on polar–optical phonons and on remote impurities in $Al_xGa_{1-x}As$.
(ii) The intersubband scattering is neglected.
(iii) Only the two lowest subbands are considerably occupied by electrons and are responsible for the impurity scattering.

The low field mobility μ_0 is composed of the two contributions, μ_{RI} (remote impurities), and μ_{PO} (optical phonons), by the Matthiessen rule

$$1/\mu_0 = 1/\mu_{RI} + 1/\mu_{PO}. \tag{20}$$

μ_{RI} is estimated from the contribution of the two lowest subbands (HOTZ, 1988) modifying therefore a theory of Hess (HESS, 1982) for a case of an interface with finite potential steps. For μ_{PO} an empirical formula

$$\mu_{PO} = A \cdot T^{-2} + B \cdot T^{-6} \tag{21}$$

(LEE et al., 1983) is used where A and B are determined by comparison with experiments.

Subsequently, a dependence of the mobility on the electric field F is introduced. This can be done easily in the expression for the drift velocity

$$v_D(F) = \mu(F) \cdot F \tag{22}$$

by a further empirical formula

$$v_{\mathrm{D}}(F) = \frac{\mu_0 \cdot F + v_{\mathrm{sat}} \cdot (F/F_{\mathrm{C}})^4}{1 + (F/F_{\mathrm{C}})^4} \tag{23}$$

(THIM, 1968). With a critical field strength

$$F_{\mathrm{C}} = 4v_{\mathrm{sat}}/\mu_0 \tag{24}$$

and measured values of the saturation drift velocity v_{sat}, the initial linear increase, the maximum, and the saturation of $v_{\mathrm{D}}(F)$ can be fitted very well. Finally, an approximation for the temperature dependence of v_{sat}

$$v_{\mathrm{sat}} = a \cdot \exp(-b \cdot T^{1/4}) \tag{25}$$

fitted to experimental values, is used (HOLZ, 1988).

Current-voltage characteristics

The simulation of the current-voltage characteristics is a two-dimensional problem. Denoting by x the co-ordinate along the channel, with $n(x,z)$ and $\mu_{\mathrm{n}}(x,z)$ also the source-drain current density

$$j_{\mathrm{n}}(x,z) = e \cdot \mu_{\mathrm{n}}(x,z) \cdot n(x,z) F_x(x,z) \tag{26}$$

depends on x and z. But averaging μ_{n} and F_x over z, the whole source–drain current is given as

$$I_{\mathrm{D}} = e \cdot \mu_{\mathrm{n}}(x) \cdot F_x(x) \int n(x,z)\, dy\, dz \tag{27}$$

and after introducing the gate width w_{G}, the electron sheet concentration $n_{\mathrm{S}}(x)$, and the drift velocity $v_{\mathrm{D}}(x)$ it takes the form:

$$I_{\mathrm{D}} = e \cdot w_{\mathrm{G}} \cdot n_{\mathrm{S}}(x) \cdot v_{\mathrm{D}}(x) \tag{28}$$

So, from (17) and (23) I_{D} can be calculated in principle in a quasi-2D manner.

Actually, U_{GS} drops along the $\mathrm{Al}_x\mathrm{Ga}_{1-x}\mathrm{As}$ layer along the channel. Therefore, for the charge control at the point x in the channel a variable amount $U_{\mathrm{G}}(x)$ is available (*Fig. 9.*).

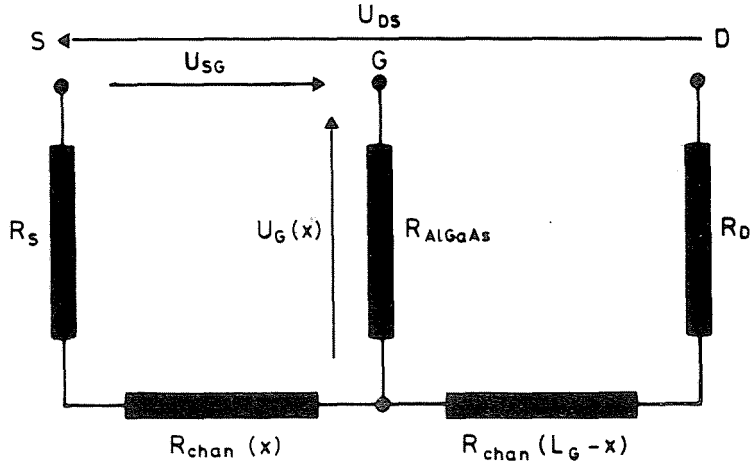

Fig. 9. Equivalent circuit for the HEMT including the resistance R_S and R_D of the contact regions

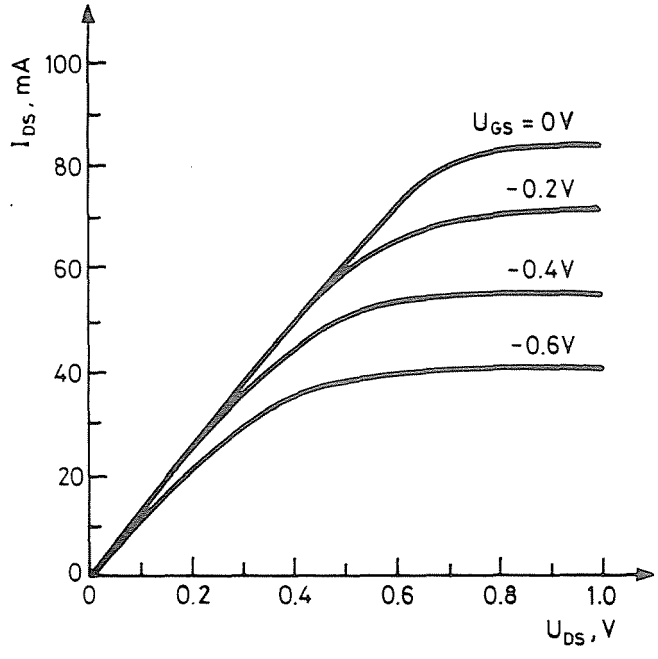

Fig. 10. Current-voltage characteristics of a normally-on HEMT (d=40 nm, d_0=0, L_G = 1μm, w_G = 200μm, $N_D = 2 \cdot 10^{18}\,cm^{-3}$, T = 77 K) for different negative values of U_{GS}

According to the drain-source voltage U_{DS} the resistances R_S and R_D of the contact regions should be taken into account. Therefore, the quasi-2D simulation of the current-voltage characteristics demands really a rather complex program for numerical calculation containing some iterative procedures (HOLZ, 1988).

As an example, in *Fig. 10.* the current-voltage characteristics of a special normally-on HEMT are given for different negative values of U_{GS}. The initial linear increase of I_{DS}, the saturation behaviour, and the charge control behaviour is very well reproduced by our simulation program without using any fitting parameters.

Now the influence of the whole set of parameters on the characteristics can be studied systematically. For instance, *Fig. 11.* shows the current-voltage characteristics without a spacer and for a spacer thickness of 4 nm. It is visible that the saturation is lower and the slope of the initial part of the curve is larger if there is a spacer.

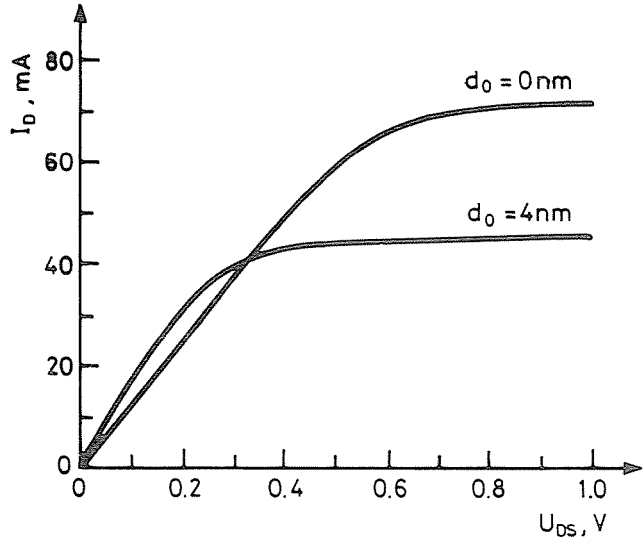

Fig. 11. Influence of a spacer on the current-voltage characteristics of a normally-on HEMT with $U_{GS} = -0.2$ V (other data as in *Fig. 10.*)

Concluding remarks

The method of HEMT simulation described in this paper can be applied also to other HEMT types and even to the other semiconductor hete-

rostructures. So it is possible to consider the effects of the 2D electron gas as well as more classical effects, such as the incomplete ionization of the donors or the occurrence of a leakage current. It has been shown that the neglection of these effects, often done in more easy and more empirical simulation models, is not allowable. Some results of the simulation of the more complicated I^2–HEMT are given in (HOLZ, 1988).

References

DINGLE, R. – GOSSARD, A.C. – WIEGMANN, W. (1975): *Phys. Rev. Lett. 34.* p. 1327.

HESS, K. (1982): *Advances in Electronic and Electron Devices 52.* p. 239.

HOLZ, G. (1988): Quasizweidimensionale Modellierung des High Electron Mobility Transistor unter Berücksichtigung von Quanteneffekten. (Quasi-two-dimensional modelling of the High Electron Mobility Transistor (HEMT) with taking into account quantum effects). Theses, Technische Hochschule Ilmenau/DDR (In German)

KINOSHITA, H. – ISHIDA, T. – INOMATA, H. – AKIYAMA, M. – KAMINISHI, K. (1986): *IEEE Trans. Electron Devices ED–33.* p. 608.

KROEMER, H. (1983): *Surface Sci. 132.* p. 543.

LEE, K. – SHUR, M.S. – DRUMMOND, T.J. – MORKOC, H. (1983): *J. Appl. Phys. 54.* p. 6432.

MILLER, R.C. – GOSSARD, A.C. – KLEINMANN, D.A. – MUNTEANU, O. (1984): *Phys. Rev. B 29.* p. 3740.

MIMURA, T. – HIYAMIZU, S. – FUJII, T. – NANBU, K. (1980): *Japan J. Appl. Phys. 19.* p. L225.

MORKOC, H. – SOLOMON, P.M. (1984): *IEEE Spectrum 21.* p. 28.

PAASCH, G. (1981): Proc. 11th Internat. Symp. Electr. Struct. of Metals and Alloys. Gaußig. Editor P. Ziesche, TU Dresden/DDR p. 121.

PAASCH, G. – ÜBENSEE, H. (1982): *Phys. Stat. Sol. (b) 113.* p. 165.

SCHNITTLER, Ch. (1988): *Wiss. Zeitschrift TH Ilmenau/DDR 34.* p. 185.

STÖRMER, H.L. (1984): *Surf. Sci. 142.* p. 130.

THIM, H.W. (1968): *J. Appl. Phys. 39.* p. 3897.

TROTT, M. – SCHNITTLER, Ch. (1989): *Phys. Stat. Sol. (b),* to be published

WALUKIEWICZ, W. – RUDA, H.E. – LAGOWSKI, J. – GATOS, H.C. (1984): *Phys. Rev. B 29.* p. 4818.

Address:

Prof. Dr. Ch. SCHNITTLER and Dr. G. HOLZ
Technische Hochschule Ilmenau
Sektion PHYTEB, WB Physik
PSF 327
6300 Ilmenau
DDR